Cyclic prefix adaptation based on channel capacity of the optical wireless channel for OFDM signals in the VLC system for enhancing the throughput and to mitigate ISI

VINAY KUMAR SINGH*, U. D. DALAL
Sardar Vallabhbhai National Institute of Technology, Surat, Gujarat, India

To alleviate the effects of the intersymbol interference (ISI) in the multicarrier system it is impetus to incorporate the cyclic prefix (CP) whose length is determined by the worst channel impulse response (CIR) duration. A nearly ISI devoid communication system can be attained for CP length more than the CIR. Such a system is power and bandwidth inefficient. In the Visible light communication (VLC) system employing optical orthogonal frequency division multiplexing (O-OFDM) the effect of such an ISI would deteriorate the received signal. In this paper we propose a technique of adapting the CP length as per the CIR which eliminates the ISI and further increases the bit rate in O-OFDM in VLC transmission systems. A mathematical model is developed to evaluate the optimal CP length based on the channel capacity. This proves to be computationally complex, so we then propose a simplified mathematical model based on the lower & the upper bound of the channel capacity and also on the delay spread of the channel. These techniques are then compared with the conventional predetermined CP length spanning 25% of the OFDM symbol based on signal to interference noise ratio (SINR) and the overall throughput of the system. A maximum improvement of 5.2% of throughput is obtained when the CP length based on channel capacity is adopted as compared to the CP length spanning 25% of the OFDM symbol.

(Received April 26, 2017; accepted November 28, 2017)

Keywords: Visible Light Communication (VLC), OFDM, Intersymbol Interference (ISI), Optical Wireless Channel (OWC)

1. Introduction

It is fascinating to have a spectrum that could endlessly cater the high bandwidth requirements at the customer end. The avenue granting such a gateway to the unprecedented visible light spectrum until now has just begun with. Besides illumination and communication simultaneously the Visible Light Communication (VLC) has other unique advantages like unlimited bandwidth, invulnerability to eavesdropping, and no regulation on transmit power [1]. Enriched with such incomparable attributes the VLC has led researchers and industries to venture into improvement of the same in terms of bit rates, longer distance communication, device advancements for higher switching speeds etc. Adhering to the simplicity of On-off keying (OOK), application in VLC [2] reports data rates upto 3Gbps by utilizing LEDs which are engineered to sustain such high speeds [3]. The mitigation of the ISI in the OFDM with VLC has also been reported in literature leading to high spectral efficiency [4]. The time domain signal intended for transmission in VLC using Intensity modulated-Direct detection (IM-DD) has to be non-negative and real valued [5]. However the enhancement of the bitrates in the system utilizing the IM-DD is limited to the switching speed of the electro-optical conversion by the LEDs. Techniques that could escalate concomitantly the electro-optical conversion are reported in [6]. By imposing the Hermitian symmetry [7] and applying a sufficient DC (Direct Current) bias to the time domain signal it is possible to obtain waveforms that are non-negative and real at the same time. Mathematically these were described in [8] and by virtue they are called the Direct Current Optical OFDM (DCO-OFDM). Modifying the OFDM such that the alternate subcarriers carry information and clipping off the negative signals also results in time domain signals that fulfill the duo-requirement of the IM-DD. These are the Asymmetrically clipped Optical OFDM (ACO-OFDM) [9].The DCO-OFDM is spectrally efficient and the ACO-OFDM is power efficient [9]. In the state of the art, the technological advancements in the multicarrier systems, Discrete Multitone-DMT and employing orthogonal subcarriers, Orthogonal Frequency Division multiplexing –OFDM provide data rates that are tens of Gbps in the wired and wireless scenario[10,11]. The need for such high rates with high spectral efficiency is essential for mostly applications like live video streaming in HD, DVB-T or even the Wireless Gigabit with Advanced Multimedia (WIGWAM) [12] within a limited bandwidth. The 4G systems support data rates of upto 100Mbps under high mobility and upto 1Gbps for nomadic movement [13].

In wireless transmission the baseband signal intended for transmission is branched into narrower data sets multiplexed over subcarriers which are robust to multipath. Maximizing the system performance involves the optimization of the available resources. The resource allocation problem namely the bit loading, power assignment and subcarrier number [14-16] are limited to a particular size of the constellation. Merely increasing the data rate has another implication which poses a time dispersion effect that could extend over long symbol intervals in the multicarrier scenario. This is averted by the addition of the cyclic prefix (CP) to the individual symbols. It serves as a guard band avoiding the Inter symbol Interference (ISI) and usually has a length just enough to be more than the longest channel impulse response (CIR). An overlooked provision for optimizing the system performance is the duration (time/samples) of the CP. Conventionally the CP length is fixed to just more than the CIR which proves to be more bandwidth and power inefficient. At the expense of avoiding the ISI it may become inevitable to have long CP in communication channels with longer CIR than usual thereby thrusting a demand on the bandwidth. In such a case the bandwidth efficiency would seemingly be low. Various techniques have been proposed to address this problem [17-19]. The transmission energy required for OFDM increases upon addition of such a prefix. The rate also declines by a ratio of the time duration of the OFDM symbol (excluding the CP) to the total duration of the OFDM symbol.

For CIRs that are time varying and dynamic, the CP length calculations for optimality becomes a point of concern. It would be advantageous to vary CP lengths according to current channel conditions. It is also noteworthy that the CP length need not be equal to the CIR in order to maximize the capacity always, as a tolerable amount of ISI may be unremarked such that the CP can be shortened. This may improve the overall system performance. Finite impulse response time domain equalizers are applied to DMT receivers for shortening the length of the CIR [18-20].Unlike equalization in the time domain [21] proposes the frequency domain equalization to each tone using a multitap. The distortions occurring due to inadequate CP can be removed by a precoder as reported by [22]. A unique technique of eliminating totally ISI and Inter Carrier Interference (ICI) was shown in [23] by combining the unused carrier samples. Another method is to implement an iterative cancellation, such as the residual ISI cancellation (RISIC) method, to remove the ICI and ISI because of the limited CP [24,25]. The magnitude of the interference caused due to the channel echoes more than the CP were calculated in [26]. It provided the solution to this problem by applying subcarrier equalization and coding in Digital TV broadcast. Simulative proofs were demonstrated in [27] that the interference is an additive white Gaussian noise (AWGN). [27] also gave the detailed study of the deterioration of the link performance in the UMTS channel model due to such interference. The capacity of the single user wireless OFDM depending upon the CP length in urban and suburban environments for 20MHz bandwidth was reported in [28]. Adaptation of the CP length in Wireless local area network (WLAN) using OFDM is investigated in [29]. The outcome suggest that the keeping the CP length as long as twice the channel delay spread would mitigate the effect of ISI. The technique of maximizing the capacity here in this work w.r.t the CP length is not complex as shown by [21] which are achieved with a complete modification of the receiver involving time domain equalization. A power penalty is inherent for the precoder implemented transmitter as reported in [22]. As per our analysis a precoder is not required as the CP length can be varied as per the channel characteristics dynamically. The overhead on power requirement thus becomes inexistent. The bandwidth inefficiency is combated in this work by using more number of subcarriers with optimal CP length to form the OFDM symbol unlike [23] where some numbers of subcarriers are left unused. The CP reconstruction method in [24,25] gives a satisfactory performance of the symbol error rate only after a number of iterations. In the method proposed by us the requirement of such an iterative process is not needed. Further, the bandwidth efficiency is enhanced by keeping the CP length to an optimum so that the ISI could be mitigated unlike in [29] where the CP is twice as long as the CIR.

In this work we present a mathematical model and perform numerical analysis on the CP length adaptation for optical signal transmission in Optical Wireless Channel (OWC). Within the indoors, where intention is to have high bit rates, the vicinity is more or less static. Thus the indoor channel would not vary much resulting in the channel to be quasi-static. The variations of the channel on time scale in fact do not change much over multiple symbol periods. Even though the channel here does not get much affected by the multipath fading, it suffers from dispersion which inherently leads to ISI. The motivation to this research lies in significantly reducing the ISI effect of the multipath components in the OWC and as a result enhancing the bit rate of the VLC system by optimizing the CP length. Within a given frame of time it is possible to incorporate more OFDM symbols in the vacant time slots that are created as a result of shortening the CP length to an optimal value. We show the dependence of the achievable rate on the CP length. Hence by maximizing the capacity we can obtain an optimal CP length. Another computationally simpler approach of evaluation is by bounding to lower and upper limits keeping the CP length as the constraining parameter. To the best of our knowledge, such techniques of optimizing the time varying CP length resulting in enhancement of the bit rate in a VLC OFDM system is surveyed first time. We report results based on mathematical derivations of the optimality conditions with an improvement of 5.2% in the bit rate of the OFDM in VLC system. The simulations are performed in Matlab.

The rest of the paper is organized in the following manner: Section 2 gives the system description in detail. The optimization of the CP length is discussed at large in Section 3. Based on the Channel capacity depending on the CP length the maximum value is determined. Following this, a relatively relaxed method of bounding the capacity to lower and upper bounds also gives a range of the CP length. We also find the optimal CP length as per the delay spread of the channel. Based on the metrics derived the numerical simulations and results are shown in Section 4. Section 5 concludes the paper with the summarization of the inferences drawn from the analysis.

2. Theoretical Analysis

We consider an OFDM signal with the number of subcarrier $= M$. The standard OFDM signal in time domain is given as,

$$s_B(t) = \frac{1}{M}\sum_{m=0}^{M-1} C_m e^{j2\pi f_m t}. \quad (1)$$

The normalized subcarrier frequencies are defined at $\frac{m}{M}$ intervals, M denotes the number of tones in the OFDM signal ($M \leq N$). The CP length is $\upsilon = N - M$ where N is the normalized subcarrier symbol period with T being the sampling time. After the electro-optical conversion by the LED, the OFDM signal is transmitted through the OWC. The current generated equivalent to the time varying OFDM signal is denoted by $\hat{I}s_B(t)$. It is ensured that the time varying current signal is positive throughout in order to avoid the turning off of the LED. It is ensured that the actual OFDM signal is real and non-negative by imposing the Hermitian symmetry while implementation. ACO-OFDM and DCO-OFDM are two well know versions of the same [28]. The total current passing through the biased LED keeping it always on can be written as

$$I_{OFDM}(t) = I_{bias} + \hat{I}s_B(t), \quad (2)$$

where $I_{bias}$is the additional DC bias applied to the elctro-optical converter. Considering the fact that the LED is a non linear device, the equivalent optical power generated on the application of the input OFDM time varying signal can formulated as

$$P_{out}(t) = \sum_n \beta_n [I_{OFDM}(t) - I_{bias}]^n, \quad (3)$$

where β_n is the co-efficient of the LED non-linearity and n is the order of the non-linearity in the LED. The optical signal is transmitted through the OWC whose equivalent discrete time impulse response is [30]

$$h(t) = \frac{A_r(m_l+1)}{2\pi d^2} cos^{m_l}(\phi) g(\psi) \cos(\psi)\, \delta(t-\theta), \quad (4)$$

where A_r denotes the aperture area of the detector, d is the channel length, m_l is Lamberts mode number that expresses the directivity of the source beam, the angle of transmission from the normal at the emitting surface is denoted by ϕ, ψ is the incidence angle of the radiation, $g(\psi)$ is the gain of the associated receiver optics and θ is the ratio of the channel length and the velocity of light in vacuum. Since most of the parameters in the CIR above are typically constant without loss of generality, we may simply assign $\rho = \frac{A_r(m_l+1)}{2\pi d^2} cos^{m_l}(\phi) g(\psi) \cos(\psi)$ yeilding,

$$h(t) = \sum_{\theta=0}^{\mu-1} \rho_\theta \delta(t-\theta). \quad (5)$$

$\delta(.)$ and $\delta(t-\theta)$ are the is the Dirac delta function and the signal propagation delay for all the possible multipath arrivals, respectively. For an indoor scenario of a simple LOS transmission (denoted by h_{LOS}), we may evaluate the received power based on the relation

$$P_r(t) = P_{out}(t) * h_{LOS}(t). \quad (6)$$

Fig.1 shows a block schematic of the implemented system. The constellation diagram from the binary data is accomplished by the quadrature amplitude mapping. The system shows the addition of the CP to the OFDM to avoid ISI. An additional DC bias to keep the LED switched on throughout the operation is also depicted. The OWC channel contains line of sight (LOS) and multipath components as well.

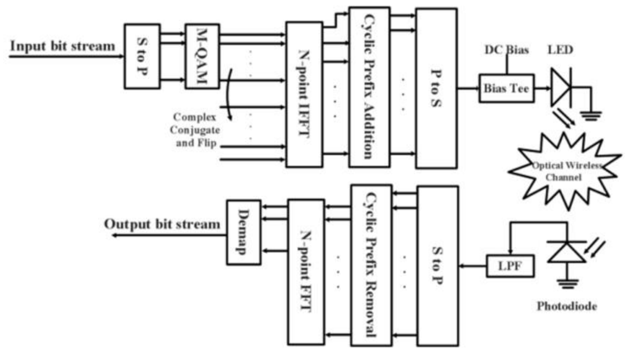

Fig. 1. Block schematic of the Optical OFDM in VLC

For analyzing the effect of the CP length modification for the OWC, we need to revamp the variables that are implicitly independent of υ in the equation (6). For the channel to be not longer than the OFDM symbol duration we assume $\upsilon \leq M$. Practically the CP length may become shorter than the CIR for harsher conditions. Nevertheless, as a result at the receiver, applying the symbol synchronization, followed by removal of the CP and performing the Discrete Fourier Transform (DFT) the time domain signal for the subcarrier m becomes

$$r_B(\ell, t) = s_B(\ell, t) * h(\upsilon, t) + i(\upsilon, \ell) + n(\ell), \quad (7)$$

where $s_B(\ell, t)$ is the ℓ^{th} data subcarrier at m, $h(\upsilon, t)$is the channel transfer function for the OFDM symbol, $i(\upsilon, \ell)$ is the ISI term and $n(\ell)$ represents the added noise. The term indicating the interference surfaces as a consequence of loss of orthogonality. The dependence on the CP length of $h(\upsilon, t)$ and $i(\upsilon, \ell)$ is explicit. The Signal to interference noise is then given by the relation

$$SINR(\upsilon) = \frac{\mathcal{P}_{s_B}(\upsilon)}{\mathcal{P}_n + \mathcal{P}_i(\upsilon)}, \quad (8)$$

where $\mathcal{P}_{s_B}$is the power corresponding to the intended data signal, $\mathcal{P}_i$ denotes the inseparable interference, and $\mathcal{P}_n$ is the additive white noise power terms on the m th subcarrier. The crosstalk between two subcarriers m and k can be formulated considering two successive OFDM symbols $h_1(t)$ and $h_2(t)$ each on m and k respectively

$$x_{h_1 h_2}(t) = (h_1(t)\, e^{j2\pi f_m t}) \otimes (h_2(t)\, e^{j2\pi f_k t}). \tag{9}$$

Then the useful signal power is given by

$$\mathcal{P}_{s_B}(v) = \mathcal{P}\left|\sum_{\theta=0}^{\mu-1} \rho_\theta (h_1(t) e^{j2\pi f_m t}) \otimes (h_2(t) e^{j2\pi f_m t})\right|^2. \tag{10}$$

The interference power

$$\mathcal{P}_i(v) = \mathcal{P}_{tot}(v) - \mathcal{P}_{s_B}(v), \tag{11}$$

where

$$\mathcal{P}_{tot}(v) = \mathcal{P}\left|\sum_{\theta=0}^{\mu-1} \rho_\theta x_{h_1 h_2}(t)\right|^2, \tag{12}$$

where $\mathcal{P}$ is the power of the constellation in the subcarrier m. The CIR in equation (5) is used to evaluate and simulate the channel behavior to implement a real world OWC. The CIR would have channel co-efficients corresponding to the LOS and non-LOS links which are separable. At the transmitter the transmit power is evaluated by equation (3). This is in time domain which is convolved with the CIR as discussed previously. The resultant is the received power given by equation (6). The evaluation of the system performance based on this received power would be incomplete as the interference is not taken into account. Hence we incorporate the terms corresponding to the interference in equation (7). This interference allows us to set limits to the tolerable amount of ISI without much affecting the data rate. The balance between the allowable ISI level and the optimal CP length for that ISI has to be maintained in order to increase the data rate.

3. Cyclic prefix length optimization

We present the criteria to optimize the CP length under the assumption that the power spectral density (PSD) mask is constrained for the transmission signal. The distribution of power over the subcarriers is uniform. We keep all the subcarriers active. Assuming the OWC to be a Gaussian channel, the data rate metric can be used to assess the effect on the systems performance due to the CP length. The input signals to the Gaussian channel are independent. Thus we may infer that the ISI and ICI are Gaussian for the OFDM transmission in the OWC.

3.1. Capacity bound criterion

The maximum data rate then is given by

$$\mathcal{C}(v) = \frac{1}{(M+v)T} \sum log_2 \left(1 + \frac{\mathcal{P}\left|\sum_{\theta=0}^{\mu-1} \rho_\theta (h_1(t) e^{j2\pi f_m t}) \otimes (h_2(t) e^{j2\pi f_m t})\right|^2}{\{\mathcal{P}_n + \mathcal{P}\left|\sum_{\theta=0}^{\mu-1} \rho_\theta x_{h_1 h_2}(t)\right|^2 - \mathcal{P}\left|\sum_{\theta=0}^{\mu-1} \rho_\theta (h_1(t) e^{j2\pi f_m t}) \otimes (h_2(t) e^{j2\pi f_m t})\right|^2\}}\right) \tag{13}$$

Optimizing v within $(0,\mu)$ yields the number of samples of the CP length such that the capacity can be maximized. Upon a closer investigation of the metric in equation (13), we understand that for each of the CP value a sum and log has to be co-calculated. This becomes more complex thereby a computationally simpler approach has to be followed.

3.2. Lower and upper bound capacity criterion:

We can find optimal length of the CP by bounding the capacity metric to a lower and an upper limit as follows. Applying the Bernoulli inequality [31] to the capacity metric (13) we obtain

$$\mathcal{C}(v) = \frac{1}{(M+\mu)T} \sum log_2 \left(1 + \frac{\mathcal{P}\left|\sum_{\theta=0}^{\mu-1} \rho_\theta (h_1(t) e^{j2\pi f_m t}) \otimes (h_2(t) e^{j2\pi f_m t})\right|^2}{\mathcal{P}_n + \mathcal{P}\left|\sum_{\theta=0}^{\mu-1} \rho_\theta x_{h_1 h_2}(t)\right|^2 - \mathcal{P}\left|\sum_{\theta=0}^{\mu-1} \rho_\theta (h_1(t) e^{j2\pi f_m t}) \otimes (h_2(t) e^{j2\pi f_m t})\right|^2}\right)^{\frac{M+\mu}{M+v}}, \tag{14}$$

$$> \frac{1}{(M+\mu)T} \sum log_2 \left(1 + \frac{(M+\mu)\dfrac{\mathcal{P}\left|\sum_{\theta=0}^{\mu-1} \rho_\theta (h_1(t) e^{j2\pi f_m t}) \otimes (h_2(t) e^{j2\pi f_m t})\right|^2}{\mathcal{P}_n + \mathcal{P}\left|\sum_{\theta=0}^{\mu-1} \rho_\theta x_{h_1 h_2}(t)\right|^2 - \mathcal{P}\left|\sum_{\theta=0}^{\mu-1} \rho_\theta (h_1(t) e^{j2\pi f_m t}) \otimes (h_2(t) e^{j2\pi f_m t})\right|^2}}{(M+v)}\right) \tag{15}$$

$$> \frac{1}{(M+\mu)T}\sum log_2\left(\frac{(M+\mu)\frac{\mathcal{P}\left|\sum_{\theta=0}^{\mu-1}\rho_\theta(h_1(t)e^{j2\pi f_m t})\otimes(h_2(t)e^{j2\pi f_m t})\right|^2}{\mathcal{P}_n+\mathcal{P}\left|\sum_{\theta=0}^{\mu-1}\rho_\theta x_{h_1h_2}(t)\right|^2}}{\frac{-\mathcal{P}\left|\sum_{\theta=0}^{\mu-1}\rho_\theta(h_1(t)e^{j2\pi f_m t})\otimes(h_2(t)e^{j2\pi f_m t})\right|^2}{(M+\upsilon)}}\right). \tag{16}$$

Further expanding the inner products,

$$\mathcal{C}(\upsilon) > \frac{M}{(M+\mu)T}log_2\left(\frac{\min\left(\mathcal{P}\left|\sum_{\theta=0}^{\mu-1}\rho_\theta(h_1(t)e^{j2\pi f_m t})\otimes(h_2(t)e^{j2\pi f_m t})\right|^2\right)}{\mathcal{P}_n}\right) -$$

$$-\frac{M}{(M+\mu)T}log_2\left(\frac{(M+\upsilon)}{(M+\mu)M}\sum\left(1+\frac{\mathcal{P}\left|\sum_{\theta=0}^{\mu-1}\rho_\theta x_{h_1h_2}(t)\right|^2-\mathcal{P}\left|\sum_{\theta=0}^{\mu-1}\rho_\theta(h_1(t)e^{j2\pi f_m t})\otimes(h_2(t)e^{j2\pi f_m t})\right|^2}{\mathcal{P}_n}\right)\right). \tag{17}$$

The optimal length of the CP in the interval $0 \le \upsilon < \mu$ is then given by minimizing the argument $(M+\upsilon)\left(M\mathcal{P}_n+\mathcal{P}\left|\sum_{\theta=0}^{\mu-1}\rho_\theta x_{h_1h_2}(t)\right|^2-\mathcal{P}\left|\sum_{\theta=0}^{\mu-1}\rho_\theta(h_1(t)e^{j2\pi f_m t})\otimes(h_2(t)e^{j2\pi f_m t})\right|^2\right)$.

The channel capacity for the upper bound can be similarly deduced as

$$\mathcal{C}(\upsilon) \le \frac{M}{(M+\upsilon)T}log_2\left(\frac{\frac{\mathcal{P}\left|\sum_{\theta=0}^{\mu-1}\rho_\theta(h_1(t)e^{j2\pi f_m t})\otimes(h_2(t)e^{j2\pi f_m t})\right|^2}{\mathcal{P}_n+\mathcal{P}\left|\sum_{\theta=0}^{\mu-1}\rho_\theta x_{h_1h_2}(t)\right|^2}}{\frac{-\mathcal{P}\left|\sum_{\theta=0}^{\mu-1}\rho_\theta(h_1(t)e^{j2\pi f_m t})\otimes(h_2(t)e^{j2\pi f_m t})\right|^2}{M}}\right) \tag{18}$$

resulting in the optimal CP length by maximizing the argument

$$\left\{\frac{\frac{\mathcal{P}\left|\sum_{\theta=0}^{\mu-1}\rho_\theta(h_1(t)e^{j2\pi f_m t})\otimes(h_2(t)e^{j2\pi f_m t})\right|^2}{\mathcal{P}_n+\mathcal{P}\left|\sum_{\theta=0}^{\mu-1}\rho_\theta x_{h_1h_2}(t)\right|^2-\mathcal{P}\left|\sum_{\theta=0}^{\mu-1}\rho_\theta(h_1(t)e^{j2\pi f_m t})\otimes(h_2(t)e^{j2\pi f_m t})\right|^2}}{M(M+\upsilon)}\right\}$$

in the interval of $0 \le \upsilon \le \mu$.

The optimal conditions derived in equation (17,18) are computationally simpler as the logarithm term does not exist anymore and also the evaluation of the SINR is not required as the lower bound is now dependent on the interference power for different υ.

3.3. Delay spread criterion

The CP length is also evaluated based on the rms value of the delay spread for a given channel response. The delay spread is given by

$$\sigma_{channel} = \sqrt{\frac{\sum_{\theta=0}^{\mu-1}T^2(\theta-\sum_{\theta=0}^{\mu-1}\theta\rho_\theta{}^2/\sum_{\theta=0}^{\mu-1}\rho_\theta{}^2)^2}{\sum_{\theta=0}^{\mu-1}\rho_\theta{}^2}} \tag{19}$$

Typically the CP length is chosen twice more than the rms delay spread of the channel (IEEE 802.11a). The optimal CP length considering a significant portion of the energy of the CIR is captured within $\gamma\sigma_{channel}$, where γ is a scalar quantity which is greater than 0 is given by

$$\upsilon_{optimal} = \gamma\frac{\sigma_{channel}}{T}. \tag{20}$$

This technique of evaluation is the most convenient method if the channel conditions are static.

4. Numerical analysis

This section numerically validates the calculations of optimal CP length provided in section 2 and its assessment in the OWC for indoor scenario on the OFDM transmission using the parameters as listed in Table1.

Table 1. System Parameters

System Parameter	Value
OFDM Bandwidth	30MHz
Number of Subcarriers	512
OFDM subcarrier frequency spacing	58.59kHz
Information duration	17.06µs
Maximum transmission distance	10m
QAM (Q)	4
FFT size	1024

As per [32] the PSD for the visible light (viz. wavelength dependent) in the range of 400nm-700nm (visible spectrum) is assumed. If the length of the channel is large compared to the wavelength then the irradiance can be assumed to be a constant throughout the surface of the photodetector. Under such an assumption, the models described previously have to be modified and the impulse response of this simple system would then approximately be a delayed and scaled dirac delta function as in equation (5). The possibility of a multipath scenario can be considered by the light emanating from the source touching the receiver surface after a numerous number of reflections from different surfaces. The channels impulse response can be summed up as an infinite series of the multipath compositions as,

$$H(\omega) = \int_{-\infty}^{\infty} h(t)\, e^{-j\omega t}\, dt \approx \sum_{-\infty}^{\infty} h(n\Delta t) e^{j\omega n\Delta t}$$

$$= \Delta t H\left(e^{j\omega\Delta t}\right), \qquad (21)$$

where the discrete-time Fourier transform $H(e^{j\omega\Delta t})$is of the discrete-time signal $h(n\Delta t)$. Fig.2 shows the PSD of the above mentioned channel as a function of the frequency. For this response, we set the number of multipath, $n = 1,2,3,4$. It can be seen that the higher order reflections corresponding to the diffuse paths contribute majorly to the dc component of the frequency response. At other frequencies the response appears to be diminishing irrespective of the multipath number. The direct LOS component has a constant magnitude of -118.2dB for the entire frequency range. The other multipath components are not considered as their contribution is negligible. Hence in our analysis to evaluate the delay spread of the channel we consider up to a maximum of four multipath components. The maximum delay spread is given by 4* delay spread of the last multipath component.

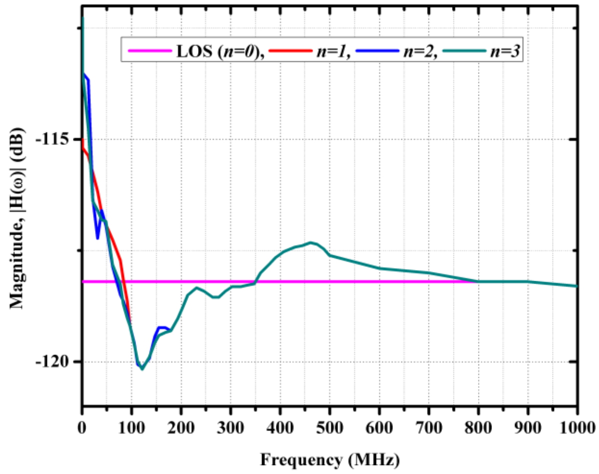

Fig. 2. Frequency response of the channel showing the magnitude of LOS and higher order reflections

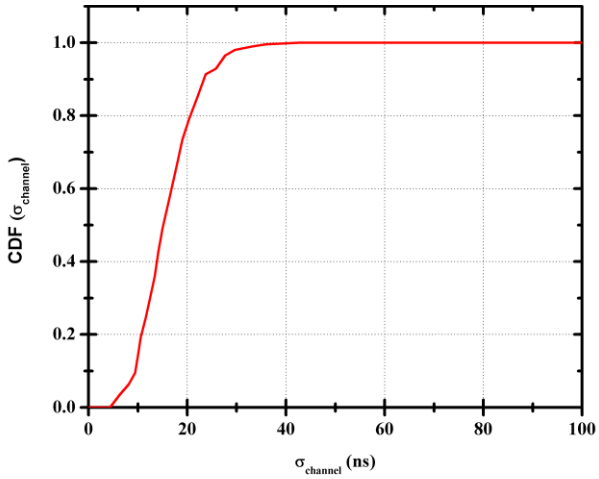

Fig. 3. CDF of the rms delay spread of the optical wireless channel

The rms delay spread measurements for the indoor OWC was performed. For this the indoor channel length was taken to be 10m (maximum).The Cumulative Distribution Function (CDF) of the rms delay spread is plotted in the Fig.3 We can notice that the rms delay spread varies significantly depending upon the channel length.

4. 1. Throughput

The bandwidth efficiency of the CP length modified system is measured by comparing the average throughput for the optimal cases. The throughput rate R at a particular signal to interference noise ratio ($SINR$) is

$$R(SINR) = \left(1 - P_e\left(\frac{\mathcal{P}\left|\sum_{\theta=0}^{\mu-1}\rho_\theta\left(h_1(t)e^{j2\pi f_m t}\right)\otimes\left(h_2(t)e^{j2\pi f_m t}\right)\right|^2}{\mathcal{P}_n+\mathcal{P}\left|\sum_{\theta=0}^{\mu-1}\rho_\theta x_{h_1h_2}(t)\right|^2 - \mathcal{P}\left|\sum_{\theta=0}^{\mu-1}\rho_\theta\left(h_1(t)e^{j2\pi f_m t}\right)\otimes\left(h_2(t)e^{j2\pi f_m t}\right)\right|^2}\right)\right)\left(\left\{\frac{N}{M+\upsilon_{optimal}}\right\}\left\{\frac{M*r}{(T_{OFDM\ symbol}+T_{CP})}\right\}\right)\ bps. \quad (22)$$

The simulated error rate at the $SINR$ is denoted by $P_e(SINR)$, r is the code rate, $T_{OFDM\ symbol}$ is the OFDM symbol duration and T_{CP} is the CP duration in continuous time. Fig shows the throughput performance of the system as a function of the $SINR$ for a BER $< 10^{-3}$. We consider five cases here to analyze the effect of CP length modification on the throughput. The first curve in the Fig.4 pertaining to no CP addition shows that for short distance LOS in the OWC a maximum rate of 510Mbps can be attained for high SINR. Such a system would be beneficial for a limited range only but with high probability of error thereby decreasing the entity $(1 - P_e(SINR))$ in equation (22).

Next we consider the conventional CP which spans 25% time duration of the OFDM symbol. It improves the rate significantly as the $P_e(SINR)$ reduces due to mitigation of the ISI. For this CP length the performance of the system is a tradeoff between the bandwidth requirement and the tolerable error rate. If the CIR has length more than the 25% time duration of the OFDM symbol the throughput declines significantly for low SINR as indicated by the initial slope of the curve. Implementing the lower bound optimal CP length improves the throughput by nearly 3% compared to the 25%$T_{OFDM\ symbol}$. This means that the bandwidth can be made use of more efficiently for the same signal strength requirement if the CP length is optimally chosen. The upper bound CP length gives a close about performance as the lower bound condition. In terms of SINR reduction the upper bound proves to be more advantageous than the lower bound whereas the reverse is true if the bandwidth utilization is a parameter of the choice. In this case we obtain an increase of throughput marginally only. The throughput of the system evaluated based on the delay spread CP length adaptation gives a performance in close proximity with the lower and upper bound criteria. It still lies intermediate between the upper and lower bounds for SINR between 15-22dB. The optimal CP length calculated as per the capacity of the channel in equation (13) yields the best performance out of the all the six categories of the CP length selection. The throughput is maximum for this case and is 45% better than the no CP condition, 5.2% more improved as compared to the 25%$T_{OFDM\ symbol}$. It is also enhanced by 2% and 2.2 % compared to the lower and the upper bound CP lengths and the delay spread CP length adaptation, respectively. For low SINR practically the systems maintain the improvement very closely.

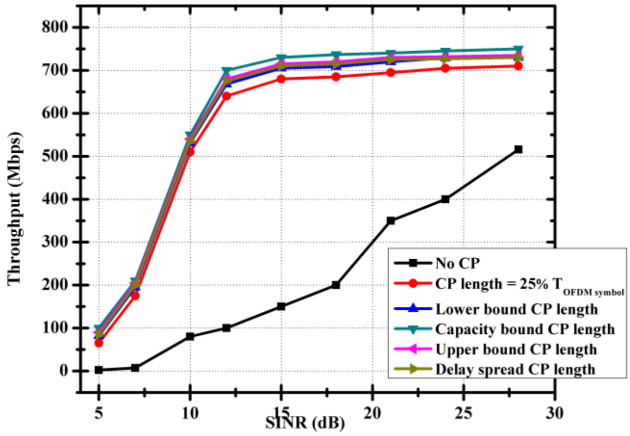

Fig. 4. Throughput vs SINR

4.2. SINR analysis

Fig. 5 shows the dependence of the SINR on the CP length. It can be observed that the SINR increases consistently with the CP length. With no CP length as indicated by point (a) in the figure the SINR is only 7dB. Although the longest CP length corresponding to equation (18) is found to be 170ns indicated by point (d) in the fig, the optimal CP length corresponding to lower bound in equation (17) is only 80ns at an SINR of 27dB. Point (c) corresponds to the capacity optimal CP length=120ns and (e) refers to the delay spread CP length both at an SINR of ~28dB. Long CP lengths lead to significant improvement in the system performance based on ISI mitigation. Thus we see that the SINR for the longest CP is highest as compared to the other two optimal CP length systems. For the general case where a fixed length corresponding to 25% of the OFDM symbol duration is taken, the SINR would be a locus of the curve plotted excluding the point corresponding to no CP.

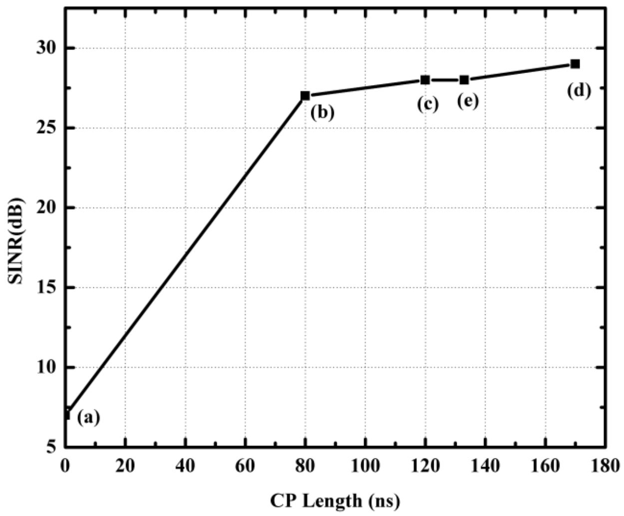

Fig. 5. SINR vs CP length

4.3. CP Length adaptation

The OFDM symbols use 512 subcarriers. The dependence of the capacity $C(\upsilon)$ on the CP length is depicted in Fig.6. The channel model is considered as described by the magnitude response in Fig.2. The channel capacity are evaluated as per equations (13,17,18,19) . We also show a case where no CP is added to the OFDM system. It can be seen that the capacity increases monotonically till a maximum is achieved corresponding to the optimality of metric (13). This optimal length was found to be 120ns in length for which the capacity was obtained around 750Mbps.If the separation between the transmitter and receiver is increased thereby increasing the attenuation, the SINR would reduce. This would mean that a higher optimal value of the CP length has to be chosen. Thus shorter CP lengths are more beneficial for channels that have low SINR requirement. The CP length for the upper bound has a lesser capacity as compared to the maximum optimal value. The overhead on the bandwidth requirement for this case is more as compared to the previous two equations (13, 17). However the effect of the ISI can be very efficiently avoided as CP lengths longer than the CIR ensure mitigation of the interference effectively. The CP length evaluated based on the delay spread criteria proves to be better as compared to the lower and the upper bound criteria. However its performance is still marginally short of the capacity optimal CP length. If we consider no CP addition case the results are more degraded. Although we expect the case to be more bandwidth efficient but the effect of ISI limits the capacity to low values. In this case for short distance communication in the OWC we obtain the theoretical value of the capacity to be in the 500 Mbps range. We may summarize that the capacity of the system with the optimized CP lengths definitely increases and indicates rate as high as 750Mbps in the VLC system.

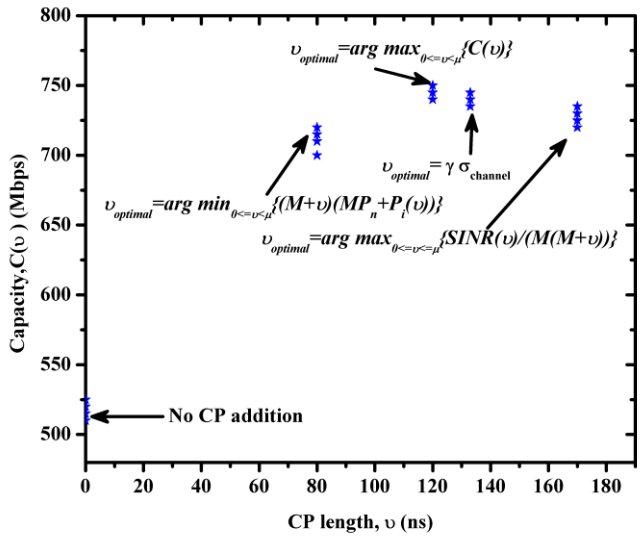

Fig. 6. Channel capacity as a function of the CP length

4.4. BER vs SINR

In the case of 4-QAM OFDM, an approximate expression for the BER is

$$BER \cong \frac{\sqrt{Q}-1}{\sqrt{Q}\log_2\sqrt{Q}}\, erfc\left[\sqrt{\frac{3\log_2 Q.SINR}{2(Q-1)}}\right] \tag{23}$$

$$\cong \frac{\sqrt{Q}-1}{\sqrt{Q}\log_2\sqrt{Q}}\, erfc\left[\sqrt{\frac{3\log_2 Q.\dfrac{\mathcal{P}\left|\sum_{\theta=0}^{\mu-1}\rho_\theta\left(h_1(t)e^{j2\pi f_m t}\right)\otimes\left(h_2(t)e^{j2\pi f_m t}\right)\right|^2}{\mathcal{P}_n+\mathcal{P}\left|\sum_{\theta=0}^{\mu-1}\rho_\theta x_{h_1h_2}(t)\right|^2} \\ -\mathcal{P}\left|\sum_{\theta=0}^{\mu-1}\rho_\theta\left(h_1(t)e^{j2\pi f_m t}\right)\otimes\left(h_2(t)e^{j2\pi f_m t}\right)\right|^2}{2(Q-1)}}\right]$$

where $erfc(x)$ is the complementary error function. The Fig.7 shows the BER against SINR for different CP adaptations. The graph shows that the BER decreases exponentially as the SINR is increased. The BER curves for the upper and lower bound criteria depict closeness in the system performance. The capacity bound CP length adapted system outperforms the other CP length adaptation techniques. The capacity bound CP length enhances the SINR performance by 1.5dB and 4.5dB as compared to the delay spread criteria and the lower and upper bound criteria respectively for the FEC threshold of BER of 10^{-3}.

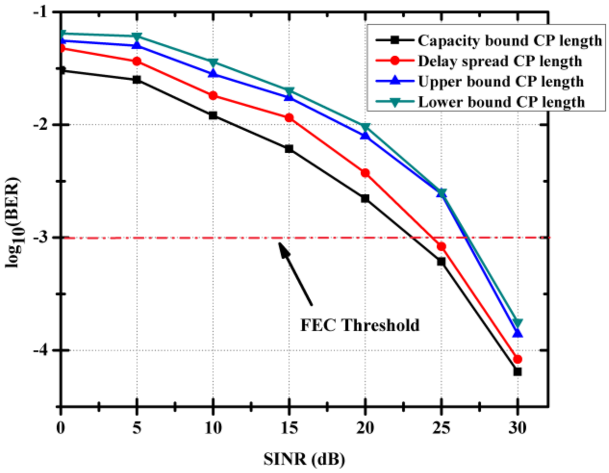

Fig. 7. BER vs SINR

5. Conclusion

An investigation of the CP length dependent curtailment of the ISI in the OFDM deployed VLC systems using the OWC is made here. We proposed that the CP length adjustments become beneficial for such communication systems. The purpose of modifying the CP length is that a significant restriction on the interference can be made in short distance quasi-static noise limited systems. We have taken into account the capacity of the system as a function of the parametric factor the optimal CP length that depends on the CIR. We find that the CP length can be capacity bound if the capacity is constrained to be CP length dependent as in equation (13). Based on the optimal CP length the corresponding capacity is obtained. A lower bound and upper bound limit to the CP length is also derived which is mathematically easier to compute than the capacity bound calculations. We also evaluate the delay spread based CP length for the channel. A comparison of no CP added and the conventional 25% time duration of OFDM symbol is also performed in terms of the throughput. Besides this, numerical results for the typical OWC channel model are used to assess the worthiness of the CP length adaptation in terms of the SINR, the throughput, and the BER. The CP length calculation takes into consideration a tolerable amount of SINR. The CP length adaptation for the capacity bound criteria gives the best result compared to the lower -upper capacity bound and the delay spread criteria in terms of the throughput and the BER performance.

Acknowledgements

The authors are thankful to Media Lab Asia, Department of Electronics and Information Technology (DEITY), for sponsoring this research work under the Visvesvaraya PhD scheme of DEITY, 2014.

References

[1] A. Jovicic, J. Li, T. Richardson, IEEE Communications Magazine **51**(12), 26 (2013).
[2] R. X. Ferreira, E. Xie, J. J. McKendry, S. Rajbhandari, H. Chun, G. Faulkner, I. H. White, IEEE Photonics Technology Letters **28**(19), 2023 (2016).
[3] J. K. Kwon, IEEE Photonics Technology Letters **22**(19), 1455 (2010).
[4] J. Armstrong, Journal of lightwave technology **27**(3), 189 (2009).
[5] S. D. Dissanayake, J. Armstrong, Journal of Lightwave Technology **31**(7), 1063 (2013).
[6] P. H. Binh, P. Renucci, V. G. Truong, X. Marie, Electronics letters **48**(12), 1 (2012).
[7] Shlomi Arnon, Cambridge University Press, 2015.
[8] J. Armstrong, B. J. Schmidt, IEEE Communications Letters **12**(5), 343 (2008).
[9] J. Armstrong, A. J. Lowery, Electron. Lett, **42**(6), 370 (2006).
[10] E. Pincemin, M. Song, J. Karaki, O. Zia-Chahabi, T. Guillossou, D. Grot, M. Van der Keur, Journal of Lightwave Technology **32**(12), 2202 (2014).
[11] A. Barbieri, G. Colavolpe, T. Foggi, E. Forestieri, G. Prati, Journal of Lightwave Technology **28**(17), 2537 (2010).
[12] J. P. Ebert, E. Grass, R. Irmer, R. Kraemer, G. Fettweis, K. Strom, E. Schulz, IEEE Communications Magazine **43**(4), 27 (2005).
[13] S. Chen, S. Sun, Y. Wang, G. Xiao, R. A. Tamrakar, China Communications **12**(2), 40 (2015).
[14] I. Kalet, IEEE Transactions on Communications **37**(2), 119 (1989).
[15] R. V. Sonalkar, R. R. Shively, IEEE Communications Letters **4**(3), 80 (2000).
[16] N. Papandreou, T. Antonakopoulos, EURASIP Journal on Advances in Signal Processing **2008**(1), 1 (2007).
[17] N. Al-Dhahir, J. M. Cioffi, IEEE Transactions on Communications **44**(1), 56 (1996).
[18] R. K. Martin, M. Ding, B. L. Evans, C. R. Johnson, IEEE Transactions on Signal Processing **52**(1), 297 (2004).
[19] C. J. Park, G. H. Im, IEEE Communications Letters **8**(9), 576 (2004).

[20] P. J. Melsa, R. C. Younce, C. E. Rohrs, IEEE Transactions on Communications **44**(12), 1662 (1996).
[21] K. Van Acker, G. Leus, M. Moonen, O. Van de Wiel, T. Pollet, IEEE Transactions on Communications **49**(1), 109 (2001).
[22] K. W. Cheong, J. M. Cioffi, IEEE International Conference, Communications, 1998. ICC 98. Conference Record. 1998 IEEE International Conference on **1**, 339 (1998).
[23] S. Trautmann, N. J. Fliege, IEEE Journal on Selected Areas in Communications **20**(5), 987 (2002).
[24] H. C. Won, G. H. Im, IEEE Communications Letters, **9**(4), 307 (2005).
[25] C. J. Park, G. H. Im, IEEE International Conference on Communications **1**, 603 (2005).
[26] E. Viterbo & K. Fazel, Global Telecommunications Conference **3**, 2069 (1995).
[27] J. L. Seoane, S. K. Wilson, S. Gelfand, Global Telecommunications Conference **1**, 32 (1997).
[28] M. Batariere, K. Baum , T. P. Krauss, Vehicular Technology Conference **l**, 543 (2004).
[29] Z. Y. Zhang & L. F. Lai, Journal of Zhejiang University Science **5**(11), 1336 (2004).
[30] Z. Ghassemlooy, Wasiu Popoola, Sujan Rajbhandari. Optical wireless communications: system and channel modelling with Matlab®. CRC Press, 2012.
[31] Eric W. Weisstein, CRC Concise Encyclopedia of Mathematics, Second Edition
[32] K. Lee, H. Park, J. R. Barry, IEEE Communications Letters **15**(2), 217 (2011).

*Corresponding author: vinayreadytochat@gmail.com